Engineering and Technology Journal

Journal homepage: https://etj.uotechnology.edu.iq

Experimental and optimization study of powder metallurgy process parameters of magnesium base AZ31 alloy using taguchi method

Basma F. Sultan[a*], **Muna K. Abbass**[a], **Jawdat A. Yagoob**[b], **Yang Y. Guo**[c]

[a] Production Engineering and Metallurgy Dept., University of Technology-Iraq, Alsina'a street, 10066 Baghdad, Iraq.
[b] Engineering Technical Collage Kirkuk Northern Technical University, Kirkuk-Iraq.
[c] Northwest Institute of Non-ferrous Metal Research, China.
*Corresponding author Email:pme.19.42@grad.uotechnology.edu.iq

HIGHLIGHTS

- Taguchi Design and ANOVA analysis were used to optimize powder metallurgy parameters.
- AZ31 alloy was fabricated using the powder metallurgy technique.
- Compaction pressure was the most impactful factor for density, porosity, and hardness at optimal settings.

ARTICLE INFO

Handling editor: Israa A. Aziz

Keywords:
AZ31 magnesium alloy
Taguchi design
ANOVA analysis
Powder metallurgy
Microstructure

ABSTRACT

Powder metallurgy (PM) is a highly effective re-processing method mostly used for magnesium-base alloys, especially in high-performance Mg alloys. In the present work, the experimental and optimization of PM process parameters, including compaction pressure, sintering temperature, and sintering time, for AZ31 magnesium alloy have been investigated using Taguchi Design of Experiment (DOE) and ANOVA method. The regression equation for obtaining density, porosity, and hardness of AZ31 Mg alloy has been formulated and experimentally validated. Three parameters are dependent in the current work, 450, 550, and 600 MPa compaction pressure, 455, 520, and 585ºC sintering temperature, and 30, 60, and 90 min sintering time. It was found that the factors determined beyond analyzing the main effect plots for means is an amalgamation of a compaction pressure (600 MPa), a temperature (585ºC) of sintering, and a time (60 min) of sintering. The optimal density, porosity, and hardness values determined from the regression equations are 1.82 g/cm^3, 3.4%, and 72.10 HV, correspondingly. The experimental density, porosity, and hardness values for the samples treated at the optimum factors are 1.73 g/cm^3, 2.2%, and 74.51 HV. The percentage error between the investigational outcomes and the outcomes resulted is < 3% for density, porosity, and hardness. The analysis ANOVA also found that the compaction pressure is the highly effective factor in the density, porosity, and hardness of sintered samples, followed by the same effective sintering temperature and time.

1. Introduction

The majority of industries, particularly vehicles, space, and aircraft, seek lightweight structural material so that the automobiles' general weight can be decreased and the capacity of payload can be augmented [1-4]. Also, Magnesium is absorbable (can be degraded safely within the body) [4,5]. Due to these extraordinary properties, demand for Magnesium and its alloys is increasing exponentially in almost all industries, i.e., automobile, aerospace, bio-medical, electronic devices, etc. With the increasing demand, there is high pressure on the natural sources of Magnesium (extraction of Magnesium from ores) [6]. Different traditional magnesium alloys that evolved from the Mg-Al–Zn ternary regime (that means the as called AZ alloys) have obtained the biggest no. of manufacturing uses. The main traditional AZ alloy grades are (AZ31, AZ61, and AZ91), which is manufactured either in the form of wrought alloys (for example, plates, sheet, extrusions, and forgings) or in the form of cast alloys (for example, sand, mold castings, and die). Generally, since the content of the aluminum alloy rises, the yield and maximum tensile strengths, resistance to corrosion, and oxidation resistance the whole rise [6]. Technologically, the most commonly used magnesium alloy is AZ31, which includes 3% Al and 1% Zn by weight. It's utilized for producing wrought products, like plates and sheets, in addition to shapes, extruded forms, and bars. The comparatively lower content of Al permits

http://doi.org/10.30684/etj.2023.142510.1539
Received 30 August 2023; Received in revised form 12 November 2023; Accepted 13 November 2023; Available online 28 January 2024
2412-0758/University of Technology-Iraq, Baghdad, Iraq

higher ductility at hot working temperatures and reinforces its matrix via solid-solution treatment [7]. Also, the AZ31 alloy is the famous Mg alloy with Al owing to its lower density and virtuous mechanical characteristics. Such structural material provides a substantial perspective for the production manufacturing of aircraft. The AZ31 alloy is employed in the aircraft industry for producing flat components with ribs-like brackets. Additionally, AZ31 Mg alloy from the set Mg-Al-Zn, described via virtuous plasticity, has been broadly used. Such alloys are intended, for example, into components with small loads, like brackets in the flying controls of aircraft [8]. Zn is being supplemented to the MgAl alloys in minor quantities further to increase the strength via solid-solution treatment. In general, AZ31 alloy is regarded as a non-heat treatable alloy [9]. The ratio of less-density elevated strength: weight of Mg causes a huge rise in the request for Mg-based materials [10]. With the rise in requests for Mg alloys and composites, there's a crucial requirement for an effective re-processing method. Traditional re-processing methods (Casting) possess less material use (approximately 50%) and elevated energy usage. Investigators globally are operating upon the evolution of a more effective re-processing method. Powder metallurgy (PM) is a highly effective re-processing method for metallic materials. PM provides different benefits over other procedures, like easy handling, elevated governing on density, low power usage, less needed machining, near-net-shape components, less scrap, elevated use of material, and so on [11, 12]. In the method of PM, mixed powders are compacted at elevated pressure to produce green compacts, and such compacts are then sintered to produce the eventual material [13]. The factors, like the pressure of compaction, the temperature of sintering, and the time of sintering, are too significant in the PM procedure. Such factors possess an elevated influence on the PM parts' properties [14]. Durai et al. [15] studied the sintering temperature influence on the properties of Mg-Zr alloy.The hardness and strength were augmented by raising the temperature of the sintering. Ma et al. [16], investigated the influence of the time of sintering upon the properties of neat Mg. The hardness augmented, and the wear rate reduced upon raising the sintering time. And, there isn't plentiful literature accessible on the Mg-based materials re-processing via the procedure of Burke and Kipouros reported a review of the re-processing and foaming of Al-based materials, clarifying the various approaches of re-processing the aluminum via PM; such approaches can be utilized for re-processing the Mg-based materials [17].Alrebdi et al. [18] evolved an Al metal matrix composite employing the PM procedure. The studies employed the orthogonal array (L9) as the investigational design. The compressive strength, Vickers hardness, and density were obtained by experiments. The S/N ratio, founded upon the law of Taguchi and the no. of anomalies completed, was utilized to determine the influence of separate input factors (ANOVA). Kumar and Bharti [19], studied the suitability of powder metallurgy for recycling magnesium AZ91 alloy. Optimization of process parameters (compaction pressure, sintering temperature, and sintering time) was done with respect to the density of AZ91 magnesium alloy’s sintered because almost all the properties (i.e., physical, mechanical, electrical, thermal, etc.) of a powder metallurgy product are dependent on the sintered density. It was observed that the compaction pressure is the most influencing parameter . Magdum and Chinnaiyan [20], studied experimental investigation and optimization of AZ31 alloy during warm incremental sheet forming to study fracture and forming behavior. The fracture behavior of the Mg alloy was studied using fractographs. Later, FE simulation was used to validate the strain value obtained from experimentation and investigate process parameters' effect on responses .

In the current research, optimization of PM process parameters (compaction pressure, sintering temperature, and sintering time) was done with respect to the density of AZ31 magnesium alloy's sintered because almost all the properties (i.e., physical, mechanical, electrical, thermal, etc.) of a powder metallurgy product are dependent on the sintered density. Sintered density depends on the extent of diffusion and the thermal expansion in the material. The diffusion and thermal expansion extent depends on the compaction pressure, sintering temperature, and sintering time. Where it was done, re-processing of the AZ31 Mg alloy was conducted employing Taguchi Design and ANOVA analysis methods. Also, regression equations to obtain the hardness, density, and porosity of AZ31 Mg alloy were formulated and experimentally validated.

2. Experimental work

2.1 Materials

The traditionally accessible pure Magnesium, Aluminum, and Zinc powders were provided via China Jingan Chemicals and Alloy Ltd. Company. Some properties of the used powders are depicted in Table 1. Particle size distribution was examined by using Smoluchowsk particle size analyzer.

2.2 Method

A subtle precise electronic balance (kind OHAUS-model 250 g-USA) with an accuracy of (0.1 mg) was employed for weighing (96 gm) of the powder of AZ31. The mix was inserted with stainless steel balls with a (1:10) weight ratio, correspondingly into a container made of stainless steel (304), and the whole charge was then milled for a period of (8 hr) at a rotational speed of (175 rpm). The ball-milled powder was compressed into disc-like samples with a diameter of 15 mm. The homogeneous mixing product was compacted using. Uniaxial Hydraulic Press (KWP 80 M-Knuth-made in Germany) was employed for the pressing step. Every sample was pressed twice. Then, the samples were sintered in an electric resistance furnace (a kind of Carbolite made in UK) in an unceasingly provided argon gas stream that heated. Also, the heating rate was kept at 10°C/min, the furnace was switched off, and the samples were finally held to cool in the furnace gradually. The chemical composition of AZ31 alloy according to ASTM standard [21] and the chemical composition of AZ31 alloy prepared by PM are shown in Table 2.

Depending upon the literature review, three factors were utilized for the optimization factors: the pressure of compaction, the temperature of sintering, and time of sintering. Three levels were chosen for these three factors. Also, the used with their levels are listed in Table 3.

The method of Taguchi Design was employed to prepare the plan of experiments. Nine various amalgamations of factors utilized for the preparation of the sample depending upon the method of Taguchi DOE are displayed in Table 4.

The specimens produced after the compaction and sintering were examined to investigate the mechanical and physical properties of AZ31 alloy for the whole (9) kinds of specimens.

Table 1: Some properties of the used powders

Powder	Color	Purity%	Average particle size, µm
Mg	Grey	99.8	100
Al	Silver	99.8	60
Zn	Silver- gray	99.8	

Table 2: Chemical composition standard value and measured value of AZ31 alloy prepared by PM

Element wt%	Al	Zn	Mn	Si	Mg
Standard value [20]	2.5-3.5	0.6-1.4	0.2-1.0	0.7-1.2	Bal.
Measured value	3.1	1.2	0.6	0.02	Bal.

Table 3: The used factors with their levels

Factors	Level 1	Level 2	Level 3
The pressure of compaction, MPa	450	550	600
Temperature of sintering,ºC	455	520	585
Time of sintering, min	30	60	90

Table 4: Design of experimental data depending upon Taguchi (L9) orthogonal array

Sample No.	Pressure of compaction (MPa)	Temperature of sintering (ºC)	Time of sintering (Min)	Sample Code
1	450	455	30	A
2	450	520	60	B
3	450	585	90	C
4	550	455	60	D
5	550	520	90	E
6	550	585	30	F
7	600	455	90	G
8	600	520	30	H
9	600	585	60	I

3. Characterization, testing, and statistical analysis

3.1 X-Ray diffraction

The XRD method was used to analyze the forming phases in AZ31 alloy powders using a lab XRD-6000 Shimadzu-JAPAN equipment housed at the Ministry of Science and Technology.

3.2 Optical microscope

Optical Microscopy was utilized for characterizing the surface morphology appearance and the microstructure of the compact sintered sample observed after etching. This test was performed in the Metallurgical Lab., Department of Production Engineering and Metallurgy- University of Technology.

3.3 Hardness

The Vickers microhardness device model (VENDER, FW100) was used to measure the hardness of sintered samples, and the results were extracted from a digital screen connected to the microhardness device.

3.4 Density &porosity

Density and porosity measurements were carried out for all compact sintered samples to obtain the bulk density and the porosity by using equations (1, 2, and 3), respectively. The mass of every sample was weighed via electronic balance (type OHAUS-USA), having an accuracy of (0.1 mg). The volume of the sample was computed with the help of the measured main dimensions of a height of (10 mm) and a diameter of (15 mm) [22]:

$$\rho m = Mc/Vg \tag{1}$$

The theoretical density (ρTh) for the specimen that was measured in accordance with the Equation (2):

$$\rho Th = \sum(\rho M * XM) \tag{2}$$

The total porosity was computed in accordance with the Equation (3):

$$PT\% = (1 - \rho m/\rho Th) * 100 \quad (3)$$

3.5 Statistical analysis

Statistical analysis was done using Taguchi and Analysis of Variance (ANOVA). Taguchi's design of experiment (DOE) is a brilliant technique for designing experiments. Employing the Taguchi method, adequate information can be determined by performing fewer experiments [23]. In such a technique, the factors are classified as controllable and uncontrollable. Also, the influence of many factors at two (2) or higher levels can be investigated simultaneously utilizing such a technique. There's usually a target value for every method or product's performance property or feature. In such a technique, optimizing the influencing parameters decreases the variability around this target value. Also, the optimal factors' level can be obtained by investigating the principal influence plots for every factor.

The percentage influence of effective parameters can also be obtained by analyzing the investigational outcomes via the analysis of variance (ANOVA).

The performance properties or features of every method or product usually belong to one of the subsequent (3) classifications:

1) Bigger is the better (The target value is unlimited).
2) Smaller is the better (The target value is 0).
3) Nominal values are better (The target value is specific).

The signal-to-noise ratio (SN ratio) is a significant statistical relationship utilized in Taguchi technique for determining the optimal factors' level. The SN ratio's elevated value suggests that the signal value is high and the noise value is low. Consequently, the levels of factors that provide the ultimate SN ratio values are optimal. The statistical Equations (4,5 and 6) to calculate the SN ratios for (3) various kinds of performance features are written below [23].

For 'the bigger is better' feature:

$$\mathrm{SN} = 10\log\left[\frac{1}{n}\sum_{n=1}^{n}\frac{1}{y2}\right] \quad (4)$$

For 'the smaller is the better' feature:

$$\mathrm{SN} = -10\log\left[\frac{1}{n}\sum_{n=1}^{n}\frac{1}{y2}\right] \quad (5)$$

For 'the nominal values are better' feature:

$$\mathrm{SN} = -10\log\ (\overline{y2}\ /S) \quad (6)$$

where: N: Number of the repeated investigational tests, *y*: Performance value, S: Target value.

4. Results and discussion

4.1 Microstructure examination

The optical microscope images evinced in Figure 1 for the AZ31 sample were prepared based on the result of the optimum PM conditions of AZ31 alloy. Figures 1 A and B, 2 A and B , and 3 manifest the microstructure, SEM examination, and XRD results, respectively, for a sample of AZ31 alloy that was prepared by PM at the optimum conditions, which were 600 MPa, 585ºC, and socking time 60 min.

4.2 Density of AZ31 alloy

The specimens' density values were augmented with a rise in compaction pressure. This is due to the high-stress concentration between the powder particles in direct contact. Also, the deformation of the powder particles generates new contacts between them, and the compacted particles tend to fill the pores between them. Figure 4A indicates the relationship between density and compaction pressure. It can be seen that with increasing the sintering temperature and sintering time, as shown in Figure 4 B &C respectively, the density first increased because of the formation of effective bonds between the existing powder particles, which minimize the volume of the pores among the compacted powders' particles which in turn was detected as an increasing in the density. The highest density value of 1.73 g/cm^3 is determined in sample I. Similar outcomes were noticed by other investigators [24].

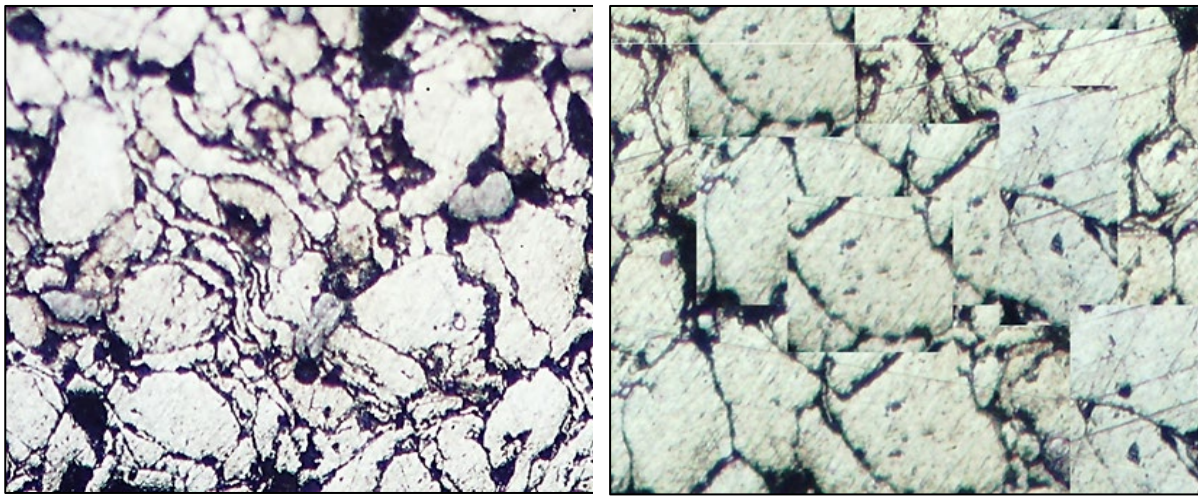

(A) (B)

Figure 1: Microstructure of the prepared base Mg AZ31 alloy at the optimum conditions (600 MPa, 585°C and 60 min) : (A) 50 µm and (B) 100 µm

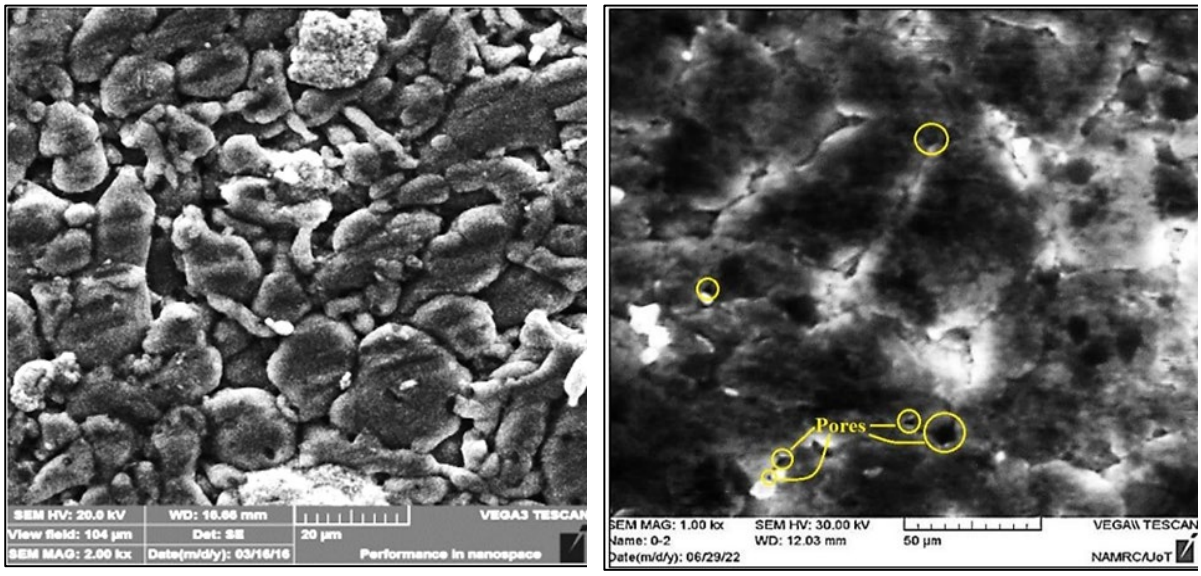

(A) (B)

Figure 2: SEM image for base alloy AZ31 for A) mixed powders AZ31 alloy and B) after sintering

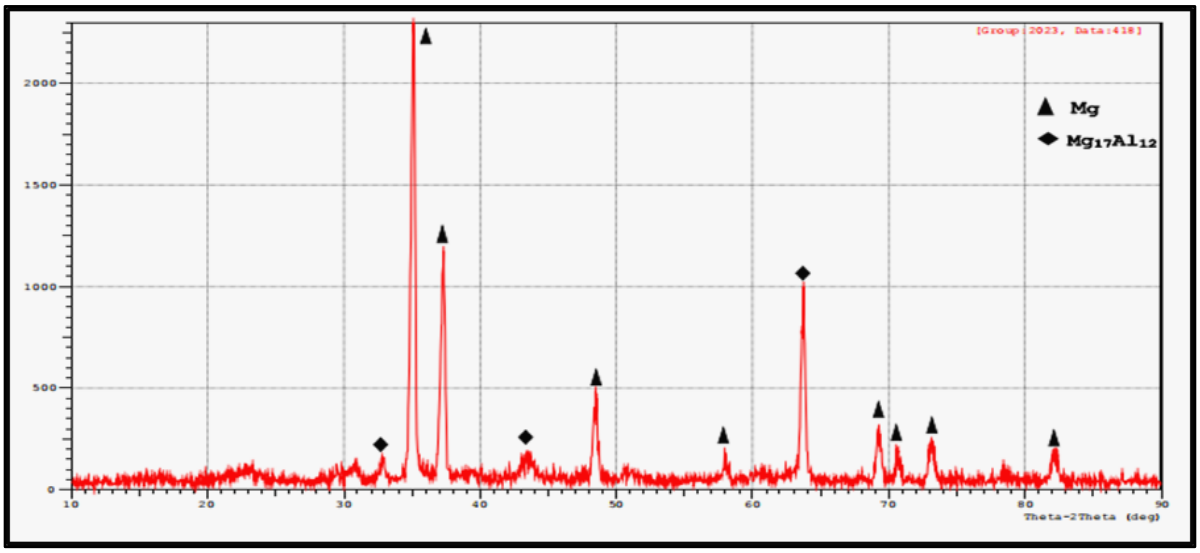

Figure 3: XRD analysis results for AZ31 alloy sintered sample

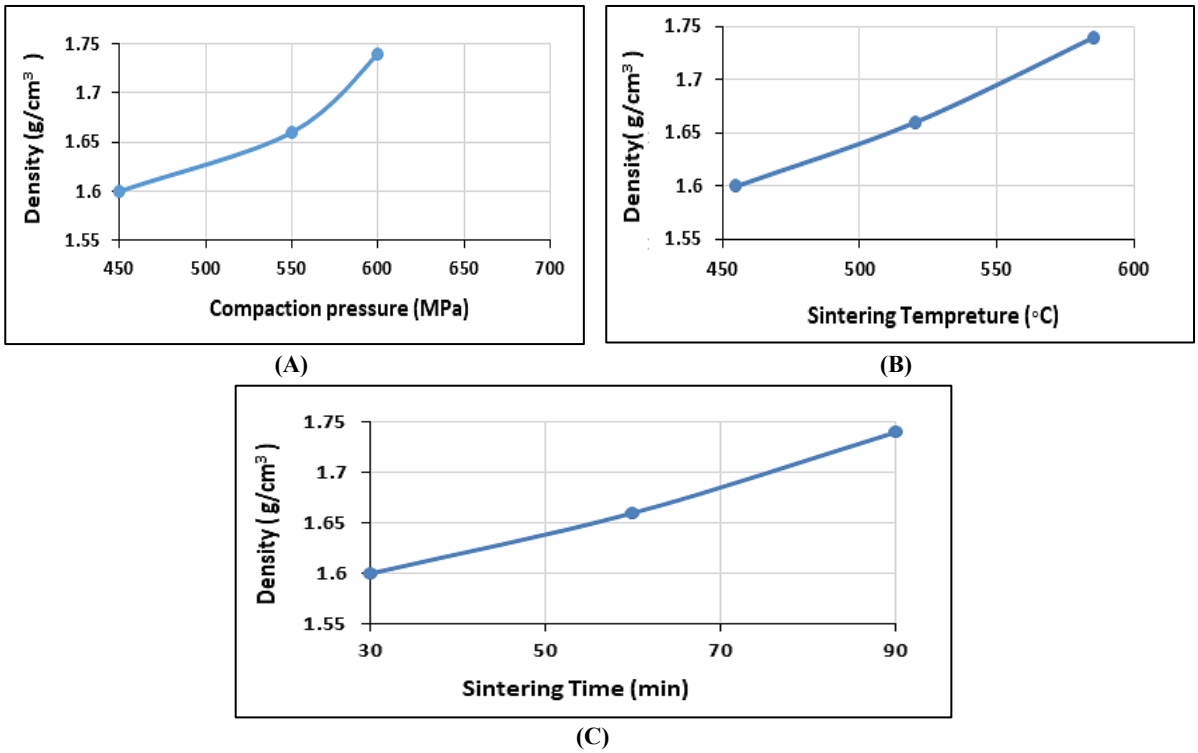

Figure 4: Relationship between Density (g/cm^3) of the compact sintered sample with (A) Compaction Pressure (MPa), (B) Sintering temperature (°C) and (C) Sintering time (min)

4.3 Porosity of AZ31 alloy

When the pressure of compaction rises, the porosity of the specimen reduces. Figure 5 A manifests the relationship between compaction pressure and porosity. Also, the porosity reduces with the temperature rise and the sintering time, as shown in Figures 5 B &C. This is due to the high densification that offers strong bonding among the particles due to the higher rate of diffusion phenomena between particles that reduce porosity. The lowest porosity value of 2.2% (0.022) is determined for sample I. Similar outcomes were noticed by other investigators [25].

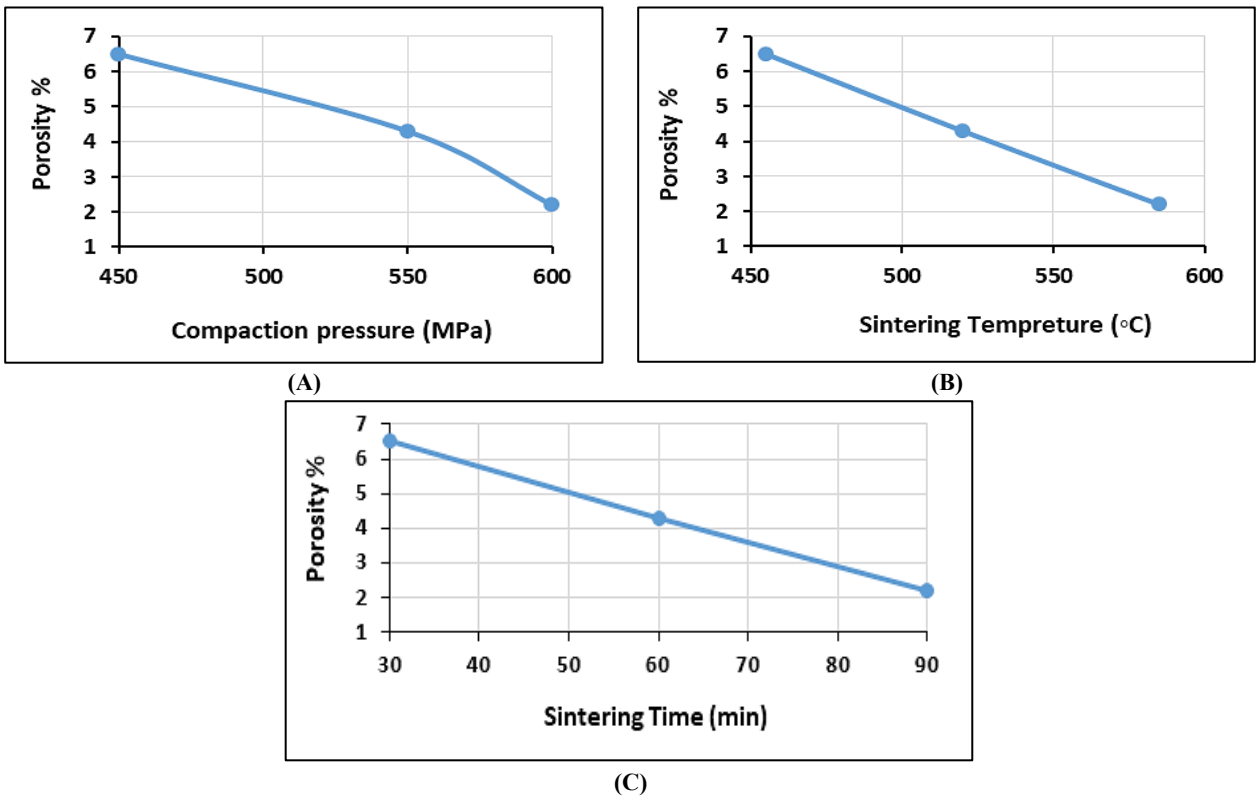

Figure 5: Relationship between Porosity% of the compact sintered sample with (A) Compaction Pressure (MPa), (B) Sintering temperature (°C) and (C) Sintering time (min)

4.4 Hardness of AZ31 alloy

The whole samples' microhardness values increase as compaction pressure increases, as shown in Figure 6 A. It can be noticed that the hardness is from 43.82 to 74.51 HV upon increased density and decreasing porosity. That is caused by values of the specimens' micro hardness augmented with a rise in the pressure compaction. This is due to the reduction of the grain's size and the densification in the sample upon raising the pressure of compression, the temperature of sintering, and the time of sintering, as shown in Figures 6 B& C. The hardness rose due to the superior diffusion bonding among the powders being determined in sample I. A similar result was seen from other investigators [26].

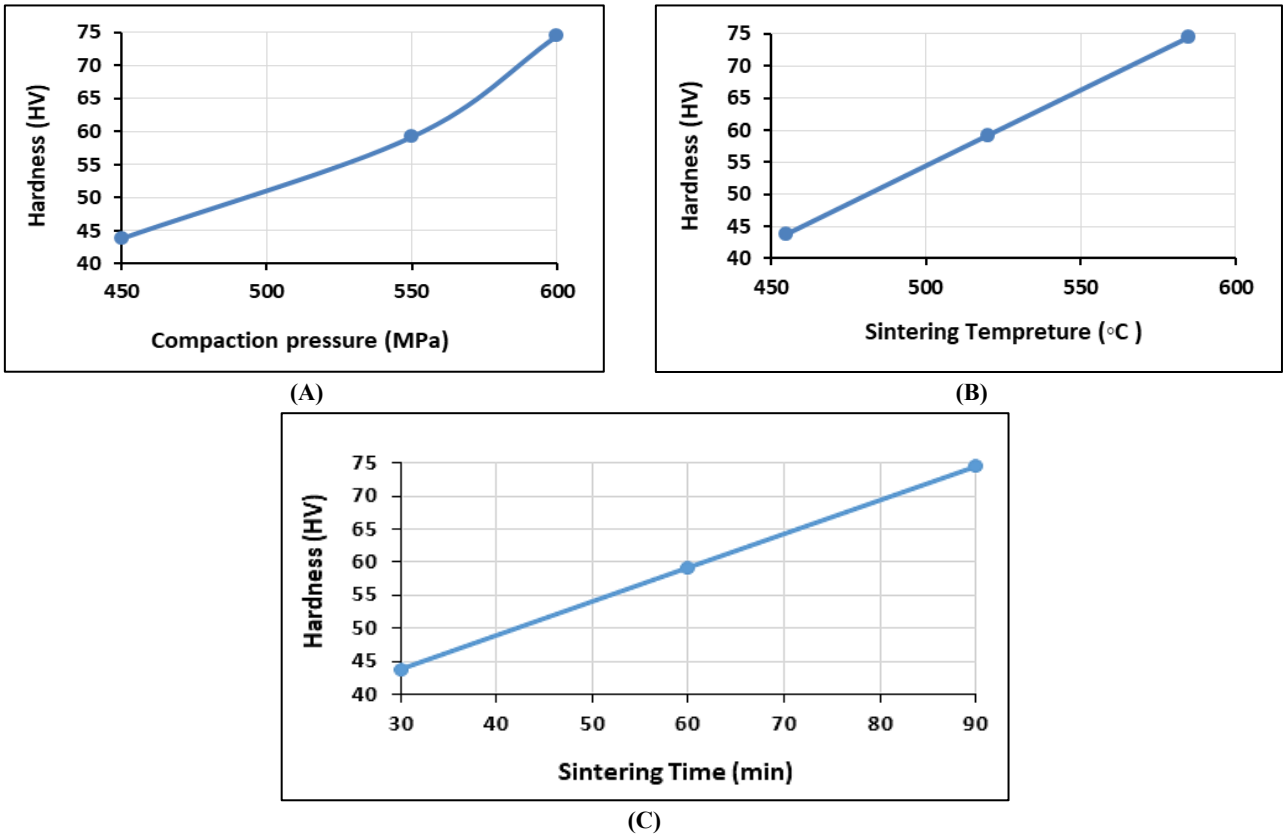

Figure 6: Relationship between Hardness (Hv) of the compact sintered sample with (A) Compaction Pressure (MPa), (B) Sintering temperature (°C) and (C) Sintering time (min)

4.5 Statistical analysis

The statistical data determined beyond the Taguchi analysis are listed in Table 5. It can be noticed that the ultimate SN ratio value for density, porosity, and hardness was determined for specimen I. This elucidates that, out of such (9) sets of method factors, the factors utilized to fabricate specimen I are the optimal method factors. Also, the plots of the main effects for means for density, porosity, and hardness are depicted in Figures 7, 8, and 9. It can also be observed from these graphs that the density and hardness unceasingly augmented with the rise in the pressure of compaction while porosity decreased.

Consequently, for the chosen (3) levels of the pressure of compaction, a (600 MPa) pressure of compaction is the optimal pressure for the re-processing of AZ31 Mg alloy, possesses a combined influence upon the density, porosity, and hardness of the prepared samples. Density and hardness initially augmented with the rise in the sintering temperature and the sintering time. But, on the other hand, the rise in the sintering temperature and the sintering time reduced the porosity because of the densification and particle boundary elimination to some extent.

Consequently, for the chosen (3) levels of the temperature of sintering and the time of sintering, the 2nd level for the temperature (585°C) of sintering and time (60 min) of sintering are the optimal method factors' levels. The optimal set of the factors of the method for the particular design will be the amalgamation of the 3rd level of the pressure (600 MPa) of compaction and 2nd level for the temperature (585°C) of sintering and the time (60 min) of sintering. The response data for the mean density, porosity, and hardness values are listed in Tables 6, 7, and 8, respectively. It can be noticed that the pressure of compaction is ranked first 1st level in the response table for the means of the density, porosity, and hardness, pursued via the second 2nd level, the same ranked temperature of sintering and time of sintering. Also, this demonstrates that the pressure of compaction is the highly significant factor in the method of PM used in the current investigation, pursued via the temperature of sintering and the time sintering.

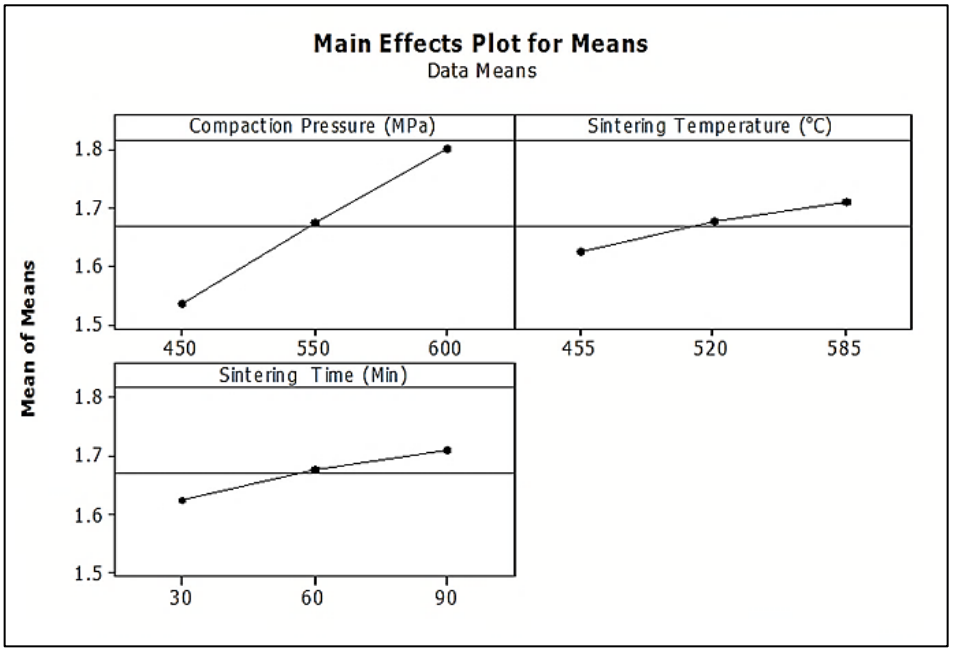

Figure 7: Main effect plots for Density

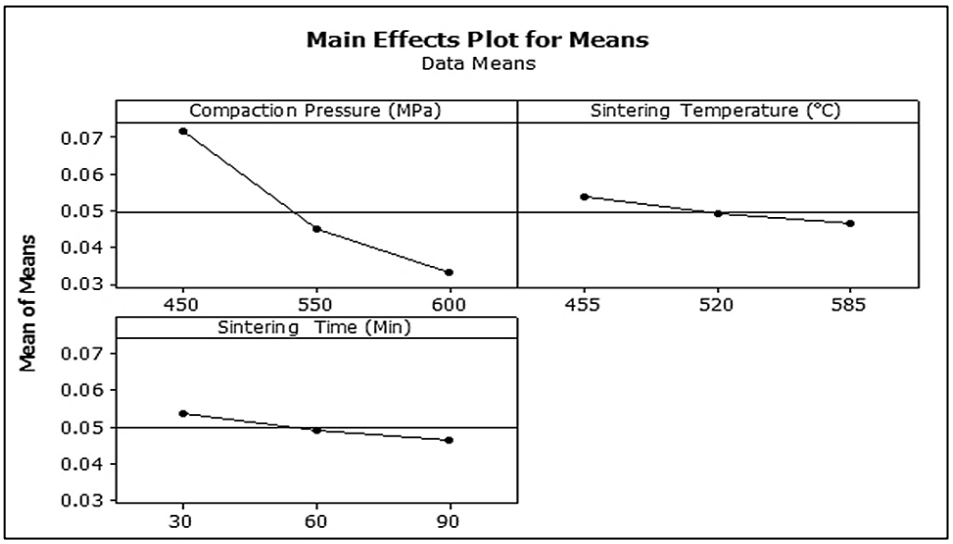

Figure 8: Main effects plots for porosity

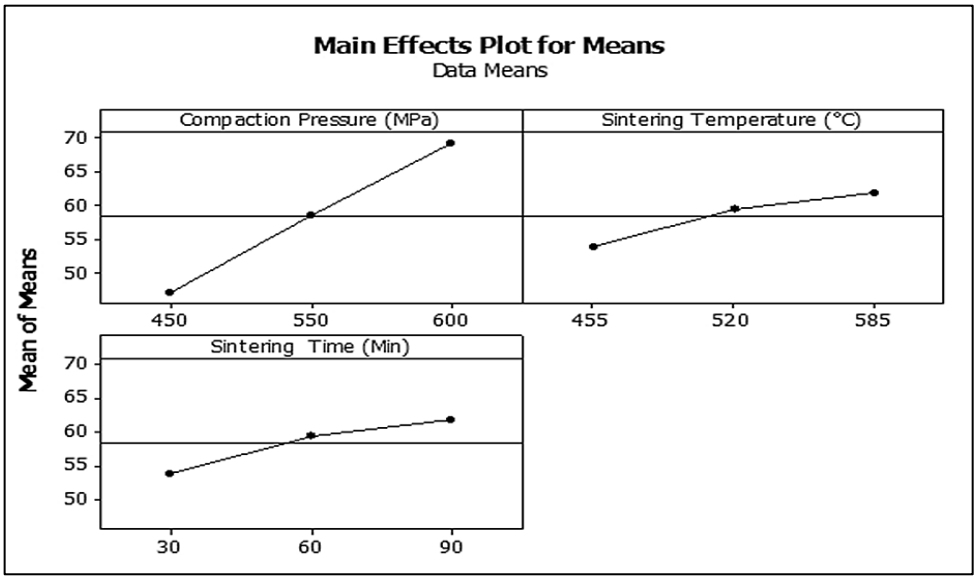

Figure 9: Main effects plots for hardness

Table 5: Statistical results for density, porosity% and hardness values

S.NO	Code	Density (g/cm^3)	Porosity	Hardness (Hv)	SN Ratio for Density	SN Ratio for Porosity	SN Ratio for Hardness
1	A	1.61	0.065	43.82	3.40523	22.4988	32.8334
2	B	1.63	0.062	47.18	3.80663	22.8534	33.4752
3	C	1.64	0.060	50.32	3.97314	23.3498	34.0348
4	D	1.67	0.053	56.26	4.13652	25.8486	35.0040
5	E	1.68	0.050	59.21	4.50619	27.3306	35.4479
6	F	1.69	0.043	60.82	4.76092	27.7443	35.6809
7	G	1.70	0.032	61.56	5.00840	29.1186	35.7860
8	H	1.72	0.025	72.45	5.10545	29.6297	37.2008
9	I	1.73	0.022	74.51	5.20143	30.1728	37.4443

Table 6: The response data for the mean Density values

Level	Compaction pressure (C)	Sintering temperature (S)	Sintering Time (T)
1	1.537	1.623	1.623
2	1.673	1.677	1.677
3	1.800	1.710	1.710
Delta	0.263	0.087	0.087
Rank	1	2.5	2.5

Table 7: The response data for the mean Porosity% values

Level	Compaction pressure	Sintering temperature	Sintering Time
1	0.07167	0.05367	0.05367
2	0.04500	0.04933	0.04933
3	0.03300	0.04667	0.04667
Delta	0.03867	0.00700	0.00700
Rank	1	2.5	2.5

Table 8: The response data for the mean Hardness values

Level	Compaction pressure	Sintering temperature	Sintering Time
1	47.11	53.88	53.88
2	58.76	59.61	59.61
3	69.51	61.88	61.88
Delta	22.40	8.00	8.00
Rank	1	2.5	2.5

Data from the analysis of variance (ANOVA) for density, porosity, and hardness are revealed in Tables 9, 10, and 11, respectively. The values of F and P in the data of ANOVA are the factors' effectiveness measures. Also, the factor having an elevated effectiveness possesses an elevated F value and low P value. Also, F-values verify the similar sequence of factor's effectiveness, as determined from the response data for density, porosity, and hardness.

The Density (D) regression Equation (7) was determined beyond the ANOVA analysis shown below. The optimal density value can be obtained by utilizing such a formula [7] by placing the optimal level value of the factors of the method in the equation. Also, the optimum density value determined from the formula employing the pressure of compaction (600 MPa), the temperature of sintering (585ºC), and the time of sintering (90 min) is 1.72 gm/cm^3.

Regression Equation:

$$D\ (g/cm^3) = 0.416667 + 0.0017 \times C\ (MPa) + 0.000666667 \times S\ (^{o}C) \quad (7)$$

Table 9: Data of the analysis of variance (ANOVA) for Density

Source	DF	Adjj SS	Adjj MS	F-Value	P-Value
Compaction pressure	2	0.104067	0.520333	111.50	0.000
Sintering temperature	2	0.011467	0.0057333	12.29	0.020
Sintering time	2	0.011467	0.0057333	12.29	0.020
Error	4	0.001867	0.0004667		
Total	8	0.117400			
S=0.02160		R-Sq=98.41%		R-Sq(adj) =96.82%	

Table 10: Data of the analysis of variance (ANOVA) for Porosity

Source	DF	Adjj SS	Adjj MS	F-Value	P-Value
Compaction pressure	2	0.0023502	0.0011751	341.16	0.000
Sintering temperature	2	0.0000749	0.0000374	10.87	0.024
Sintering time	2	0.0000749	0.0000374	1.087	
Error	4	0.0000138	0.0000034		
Total	8	0.0024389			
S = 0.001856		R-Sq = 99.44%		R-Sq(adj) = 98.87%	

Table 11: Data of the analysis of variance (ANOVA) for Hardness

Source	DF	Adjj SS	Adjj MS	F-Value	P-Value
Compaction pressure	2	753.057	376.529	56.63	0.001
Sintering temperature	2	102.077	51.039	7.68	0.043
Sintering time	2	102.077	51.039	7.68	0.043
Error	4	26.598	6.649		
Total	8	881.732			
S = 2.579		R-Sq. = 96.98%		R-Sq.(ad j) = 93.97%	

The regression Equation (8) for the porosity (P) determined beyond the ANOVA analysis is below. The optimal porosity value can be obtained by utilizing such a formula [8] by placing the optimal levels value of the factors of the method. Also, the optimum porosity value determined from the formula employing the pressure of compaction (600 MPa), the temperature of sintering (585ºC), and the time of sintering (60 min) is 0.059.

Regression Equation:

$$P\ \% = 0.216048 - 0.000259048\times C\ (MPa) - 5.38462\text{-}005\times S\ (^{o}C) \quad (8)$$

The Hardness (H) regression Equation (9) was determined beyond the ANOVA analysis displayed below. The optimum hardness value can be obtained by utilizing such a formula [9] by placing the optimal levels value of the factors of the method. Also, the optimum hardness value determined from the formula employing the pressure of compaction (600 MPa), the temperature of sintering temperature (585ºC), and the time of sintering (60 min) is 72.10 HV.

Regression Equation:

$$H\ (HV) = -50.7024 + 0.144652\times C\ (MPa) + 0.0615641\times S\ (^{o}C) \quad (9)$$

4.6 Experimental validation

The experimental validation of the outcomes resulted from the regression formulas for density, porosity, and hardness was conducted for the samples made utilizing the determined optimum factors of density, porosity, and hardness outcomes. Both the regression analysis and investigational outcomes are given in Table 12. It can be noticed that the percentage error between the investigational outcomes and the outcomes resulting from the formula of regression is < 3% for density, porosity, and hardness. Therefore, the regression formulas give satisfactory outcomes and can be utilized for determining the values of density, porosity, and hardness at the other factors' sets.

Table 12: The difference between the investigational and the regression analysis outcomes

	Density gm/cm^3	Porosity%	Hardness (HV)
Regression Result	1.82	2.9	72.10
Experimental Result	1.73	2.2	74.51
Error	1%	0.7	2.4%

5. Conclusion

The subsequent conclusions can be drawn beyond the description as well as testing of the AZ31 Mg alloy samples produced via the process of powder metallurgy (PM):

The powder metallurgy technique was successfully applied to prepare AZ31 Mg alloy produced using the optimum conditions: Compaction pressure (600 MPa), sintering temperature (585ºC), and sintering time (90 min). It was shown that the best sintering temperature was at 585°C for the compact Mg alloy (AZ31), which gave the highest density and hardness compared to other sintering temperatures. The XRD analysis manifested the existence of precipitation of second phases, Al_{12} Mg_{17} and Mg_2Zn, in the Mg alloy of the sintered alloy at a temperature of 585°C and a time of 60 min. The sample I has the highest density value (1.73 gm/cm^3), hardness (74.51 HV), and less porosity 2.2%.Out of the three selected parameters, it was obtained that the pressure of compaction is the highly effective process factor for density, porosity, and hardness, pursued via the temperature of sintering and the time of sintering time that have a similar influence. It was shown that the regression analysis results agree with the experimental results.

Acknowledgment

The researchers would like to sincerely thank the Production Engineering and Metallurgy Department at University of Technology for allowing us to accomplish such an investigation.

Author contributions

Conceptualization, B. Sultan, M. Abbass, J. Yagoob, and Y. Guo; Methodology: B. Sultan, M. Abbass, and J. Yagoob; Writing-Original Draft Preparation, B. Sultan, M. Abbass, and J. Yagoob; Writing-Review and Editing, B. Sultan, M. Abbass, J. Yagoob, and Y. Guo. All authors have read and agreed to the published version of the manuscript.

Funding

The present research has not received any external funding.

Data availability statement

The data that support the findings of this study are available on request from the corresponding author.

Conflicts of interest

The authors declare that there is no conflict of interest.

References

[1] H. Cai, F. Guo, Study on Microstructure and Strengthening Mechanism of AZ91-YMagnesium alloy, Mater. Res. Express, 5 (2018) 36-50 . https://doi.org/10.1088/2053-1591/aab0b7

[2] E. Ghasali, M. Alizadeh, M.Niazmand, and T.Ebadzadeh, Fabrication of Magnesium-Boron Carbide Metal Matrix Composite by Powder Metallurgy Route: Comparison between Microwave and Spark Plasma Sintering, J. Alloys Compd., 697 (2016) 200-207. https://doi.org/10.1016/j.jallcom.2016.12.146

[3] C.S.Goh, J. Wei , L.C.Lee,M.Gupta, Development of Novel Carbon Nanotube Reinforced Magnesium Nanocomposites using the Powder Metallurgy Technique, Nanotechnology, 17 (2006) 7-12. https://doi.org/10.1088/0957-4484/17/1/002

[4] L.F. Guleryuz , S. Ozan, D. Uzunsoy, R. Ipek , An Investigation of The Microstructure and Mechanical Properties of B4C Reinforced PM Magnesium Matrix Composites, Powder Metall. Met. Ceram., 51 (2012) 456-462. https://doi.org/10.1007/s11106-012-9455-9

[5] N.Akcamlı , B. Senyurt , Fabrication and Characterization of In-situ Al_3Ni Intermetallic and CeO_2 Particulate-Reinforced Aluminum Matrix Composites, Ceram. Int., 47 (2021) 197-206. https://doi.org/10.1016/j.ceramint.2021.04.122

[6] A.Dey, K.M.Pandey , Magnesium Metal Matrix Composites - A Review, Rev. Adv. Mater.Sci., 42 (2015) 58-67.

[7] M. Ali , M.A.Husseien and N.AL-Aqeeli ,Magnesium –based composites alloys for medical applications :A review of mechanical and corrosion properties, J. Alloys Compd., 792 (2019) 162-1190.

[8] M. peter, A. Man and G. Dias ,Magnesium and it Alloys as orthopedic biomaterials, Elsever, 27 (2006) 1728-1734.

[9] P. Burke, D. Fancelli and G. J. Kipouros, Investigation of the Sintering , Metals in Transport Applications, 48 (2009) 123-132. http://dx.doi.org/10.1179/cmq.2009.48.2.123

[10] C. Blawert, N. Hort, K.U. Kainer, Automotive applications of Magnesium and its alloys, Trans. Indian Inst. Met., 57 (2004) 397-408.

[11] D. Kumar, A. Bharti, S.M. Azam, N. Kumar, H. Tripathi, Investigations of Mechanical Properties of Copper Matrix Hybrid Composite, Adv. Mech. Eng., 46 (2020).671-676. https://doi.org/10.1007/978-981-15-0124-1_60

[12] H.Y. Wang, Q.C. Jiang, Y. Wang, B.X. Ma, F. Zhao, Fabrication of TiB_2 Particulate Reinforced Magnesium Matrix Composites by Powder Metallurgy, Mater. Lett., 58 (2004) 3509-3513. https://doi.org/10.1016/j.matlet.2004.04.038

[13] M.K. Abbass, J. A. yagoob, Effect of a-Al_2o_3 Nanoparticles Addition On Some Properties Of Cocrmo Alloy Fabricated By Powder Metallurgy Route, Iraqi J. Mech. Mater. Eng., 20 (2020) 47-62.

[14] L. Guo, H. Xin, Z. Zhang, X. Zhang, F. Ye, Microstructure Modification of Y_2O_3 Stabilized ZrO_2 Thermal Barrier Coating by Laser Lazing and Effect on the Hot Corrosion Resistance, J. Adv. Ceram., 9 (2020) 232-242. https://doi.org/10.1007/s40145-020-0363-z

[15] T.J. Durai, M. Sivapragash, M.E .Sahayaraj, Effect of Sintering Temperature on Mechanical Properties of Mg-Zr Alloy, Int. J. Mech. Prod. Eng. Res. Dev., 7 (2017) 117-122.

[16] L.Ma, P. Jin , X. Feng L.i Jia, Effect of Sintering Temperature on Microstructure and Mechanical Properties of ZK60 magnesium alloys,Mater.l Res. express., 9 (2022) 016514.https://doi.org/10.1088/2053-1591.

[17] P Burke, G.J. Kipouros, Development of Magnesium Powder Metallurgy AZ31 Alloy Using Commercially Available Powders, High Temp. Mater. Proc., 30 (2011) 51–61.https://doi.org/10.1515/htmp.2011.007

[18] T.A. Alrebdi, R. Gopinathan, P. Sunagar, R.T. Prabu, R. Kivade, M.Z .Gous, A. Alodhayb, Optimization on Powder Metallurgy Process Parameters on Nano BoronCarbide and Micron Titanium Carbide Particles Reinforced AA 4015 Composites by Taguchi Technique, J. Nanomater., 2022 (2022) 1-9 . https://doi.org/10.1155/2022/3577793

[19] N. Kumar, A. Bharti , Optimization of powder metallurgy process parameters to recycle AZ31 magnesium alloy , Material physic N Kumar, A Bharti al mechanics , 47 (2021) 968-977. http://dx.doi.org/10.18149/MPM.4762021_15

[20] R. Magdum, P. Chinnaiyan, Experimental Investigation and Optimization of AZ31 Mg Alloy during Warm Incremental Sheet Forming to Study Fracture and Forming Behavior, Coatings, 68 (2023) 2-19. https://doi.org/10.3390/coatings13010068

[21] Zhuanxin, Chemical Composition of Magnesium alloy (%) ASTM standard, and Mechanical Properties of Magnesium alloys, All kind metal material and CNC machining part and rapid prototype manufacture, Page 1.

[22] M.K. Abbass, B.F. Sultan, Effect of Al_2O_3 Nano-particles on Corrosion Behavior of Aluminum alloy (Al-4.5%Cu-1.5 Mg) Fabricated by Powder Metallurgy ,Journal Engineering Structure and Technologies ,11(2019) 1-7.

[23] J.A. Yagoob, M.K. Abbass, Characterization of Cobalt Based CoCrMo Alloy Fabricated by Powder Metallurgy Route, 2nd Int. Conf. Eng. Technol. Sci. Al-Kitab University, 2018, 1-5. https://doi.org/10.1109/ICETS.2018.8724615

[24] M.K. Abbass, B.F. Sultan, Effect Sintering Temperature on Physical Properties and Corrosion Behavior of Compact (Al-4.5wt% Cu-1.5 wt% Mg) Alloy, Iraqi J. Mech. Mater. Eng., 17 (2017) 394-407.

[25] M. Marya, L.G .Hector, R. Verma, W. Tong, Microstructural effects of AZ31 magnesium alloy on its tensile deformation and failure behaviors Mater. Sci. Eng. A, 418 (2006) 341-356. https://doi.org/10.1016/j.msea.2005.12.003

[26] A. Kumar, P.M. Pandey,Development of my Mg based biomaterials with improved mechanical and degradation properties using powder metallurgy , J. Magnes. Alloy., 8 (2020) 883-898. https://doi.org/10.1016/j.jma.2020.02.011